



Structure refinement of $(\text{NH}_4)_3\text{Al}_2(\text{PO}_4)_3$ prepared by ionothermal synthesis in phosphonium based ionic liquids – a redetermination

Christopher P. Nicholas,^{a*} John P.S. Mowat^b and Robert W. Broach^b

^aExploratory Materials and Catalysis Research, Honeywell UOP, Des Plaines IL 60201, USA, and ^bAdvanced Characterization, Honeywell UOP, Des Plaines IL 60201, USA. *Correspondence e-mail: christopher.nicholas@uop.com

Received 17 October 2019

Accepted 13 November 2019

Edited by M. Weil, Vienna University of Technology, Austria

Keywords: powder diffraction; aluminophosphate; ionothermal synthesis; ethyltributylphosphonium diethylphosphate; Cyphos 169; redetermination.

CCDC reference: 1965580

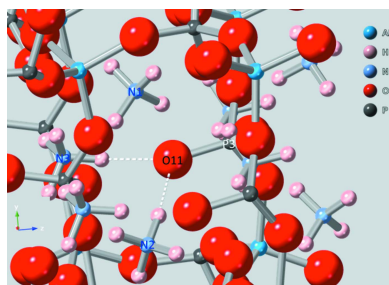
Supporting information: this article has supporting information at journals.iucr.org/e

After crystallization during ionothermal syntheses in phosphonium-containing ionic liquids, the structure of $(\text{NH}_4)_3\text{Al}_2(\text{PO}_4)_3$ [triammonium dialuminum tris(phosphate)] was refined on the basis of powder X-ray diffraction data from a synchrotron source. $(\text{NH}_4)_3\text{Al}_2(\text{PO}_4)_3$ is a member of the structural family with formula $A_3\text{Al}_2(\text{PO}_4)_3$, where A is a group 1 element, and of which the NH_4 , K , and Rb forms were previously known. The NH_4 form is isostructural with the K form, and was previously solved from single-crystal X-ray data when the material (SIZ-2) crystallized from a choline-containing eutectic mixture [Cooper *et al.* (2004). *Nature*, **430**, 1012–1017]. Our independent refinement incorporates NH_4 groups and shows that these NH_4 groups are hydrogen bonded to framework O atoms present in rings containing 12 T sites in a channel along the c -axis direction. We describe structural details of $(\text{NH}_4)_3\text{Al}_2(\text{PO}_4)_3$ and discuss differences with respect to isostructural forms.

1. Chemical context

Following the discovery of the microporous AlPO_4 - n series of materials (Wilson *et al.*, 1982), many efforts have been directed toward the synthesis of novel phases utilizing traditional hydrothermal (Wilson, 2007; Yu & Xu, 2006) and solvothermal syntheses (Das *et al.*, 2012). Recently, ionothermal synthesis has been added to the stable of synthetic methods. Ionothermal synthesis is an extension of the solvothermal method of synthesis using an ionic liquid as the solvent (replacing, for example, water or ethylene glycol) where a portion of the organic structure-directing agent from a typical zeolite synthesis is derived from the ionic liquid (Morris, 2009). Many new materials have been synthesized by ionothermal synthesis, with new aluminophosphate materials among the most common (Parnham & Morris, 2007; Xing *et al.*, 2008, 2010).

An important issue in ionothermal synthesis is control of water (Ma *et al.*, 2008). Excess water often leads to synthesis of dense AlPO_4 phases such as the one with a tridymite-type of structure, which we observed as well during syntheses utilizing 85%_{wt} H_3PO_4 . To control the level of water in the synthesis, thereby allowing easy recycling of the ionic liquid solvent and to intentionally prepare ammonium aluminophosphates, we used $(\text{NH}_4)_2\text{HPO}_4$ as the phosphorous source in the synthesis. Ammonium is a good structure-directing agent for aluminophosphate frameworks; multiple ammonium aluminum phosphates are known (Byrne *et al.*, 2009; Vaughan *et al.*, 2012). In the current phosphonium-based ionothermal synthesis, the presence of an ammonium cation in the relative absence of water provokes the formation of a 2/3 Al/P framework with



OPEN ACCESS

the formula $(\text{NH}_4)_3\text{Al}_2(\text{PO}_4)_3$. A structurally unrelated compound with the formula $(\text{NH}_4)_3\text{Al}_2(\text{PO}_4)_3$ has previously been synthesized *via* a solvothermal approach (Medina *et al.*, 2004).

The aluminophosphate database at Jilin (Li *et al.*, 2019) currently lists 21 framework structures with a 2:3 ratio of Al:P. A framework with sub-stoichiometric Al content is by necessity anionically charged and must be cation-balanced, so most of the known frameworks, such as UT-3, UT-4 and UT-5 (Oliver *et al.*, 1996) are charge-balanced by organoammonium cations. Low-water-content syntheses clearly favor 2:3 compounds as most of the known materials are synthesized from low-water-content preparations.

2. Structural commentary and survey of related compounds

The $(\text{NH}_4)_3\text{Al}_2(\text{PO}_4)_3$ phase synthesized here is related to the series of $A_3\text{Al}_2(\text{PO}_4)_3$ materials synthesized *via* high-temperature solid-state methods (Devi & Vidyasagar, 2000) with varying monocations on the *A* site. Additionally, an independent synthesis previously yielded a $(\text{NH}_4)_3\text{Al}_2(\text{PO}_4)_3$ material called SIZ-2 whose structure was solved and refined from single-crystal data (Cooper *et al.*, 2004) and possesses nearly the same structure as refined from the current powder data of $(\text{NH}_4)_3\text{Al}_2(\text{PO}_4)_3$. A polyhedral representation of the crystal structure of $(\text{NH}_4)_3\text{Al}_2(\text{PO}_4)_3$ is shown in Fig. 1. SIZ-2 crystallized from a choline chloride/urea eutectic mixture where decomposition of urea was proposed to be the source of ammonium in the structure. The refinement of Cooper *et al.* (2004) included the ammonium N atoms, but made no attempt to find or model the corresponding H atoms.

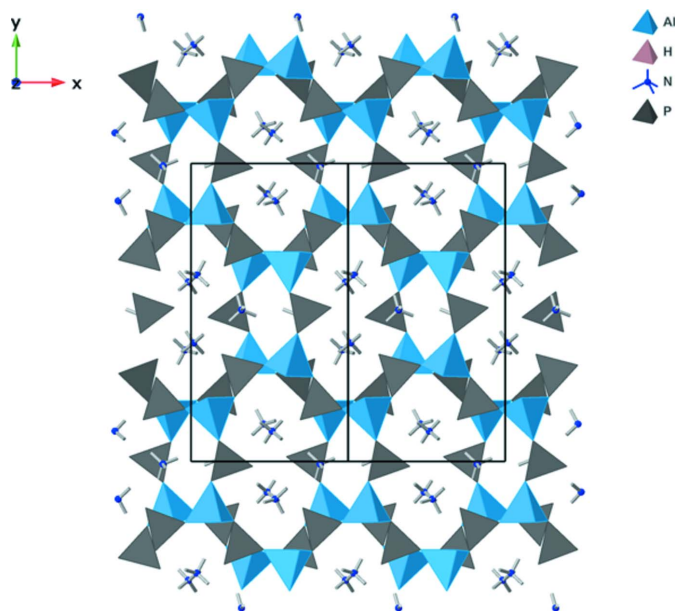


Figure 1
Polyhedral representation of $(\text{NH}_4)_3\text{Al}_2(\text{PO}_4)_3$, showing the overall connectivity and ion channels in the crystal structure. Al is in the center of blue tetrahedra, P in gray tetrahedra, and N is represented by blue spheres.

Table 1
Hydrogen-bond geometry (\AA , $^\circ$).

$D-H\cdots A$	$D-H$	$H\cdots A$	$D\cdots A$	$D-H\cdots A$
N1–H11 \cdots O9 ⁱ	0.95 (4)	2.39 (4)	3.250 (10)	151 (3)
N1–H11 \cdots O11	0.95 (4)	2.35 (5)	3.163 (8)	143 (3)
N1–H12 \cdots O1 ⁱⁱ	0.95 (4)	1.88 (4)	2.791 (10)	159 (3)
N1–H13 \cdots O5	0.95 (4)	2.14 (4)	2.934 (10)	141 (3)
N1–H14 \cdots O9 ⁱⁱⁱ	0.95 (4)	1.83 (4)	2.776 (9)	173 (3)
N2–H21 \cdots O5 ^{iv}	0.95 (4)	1.96 (4)	2.896 (10)	170 (4)
N2–H22 \cdots O8 ^v	0.95 (4)	2.31 (3)	3.216 (10)	158 (4)
N2–H23 \cdots O9 ^{iv}	0.95 (4)	1.89 (5)	2.738 (9)	148 (4)
N2–H24 \cdots O11 ^{vi}	0.96 (4)	1.86 (4)	2.818 (9)	174 (5)
N3–H31 \cdots O5 ^{vi}	0.96 (4)	1.97 (4)	2.821 (9)	147 (3)
N3–H32 \cdots O11 ^{vi}	0.952 (15)	1.85 (2)	2.728 (8)	153 (4)
N3–H33 \cdots O1 ^v	0.95 (3)	1.90 (3)	2.823 (9)	164 (4)
N3–H34 \cdots O12	0.96 (3)	2.37 (4)	2.925 (8)	117 (4)

Symmetry codes: (i) $x, y, z + 1$; (ii) $x - \frac{1}{2}, -y + \frac{1}{2}, z + 1$; (iii) $-x, -y + 1, z + \frac{1}{2}$; (iv) $x + 1, y, z$; (v) $x + \frac{1}{2}, -y + \frac{1}{2}, z$; (vi) $-x + 1, -y + 1, z - \frac{1}{2}$.

Devi & Vidyasagar (2000) utilized Li, Na, K, Rb, Cs, and Tl as the *A* cation and succeeded in crystallizing compounds with $A = \text{Na}, \text{K}, \text{Rb}, \text{Tl}$. The thallium derivative yielded a completely different structure with trigonal-bipyramidal coordination of Al. The $A = \text{Na}$ structure was not solved, but apparently crystallizes in an unrelated orthorhombic space-group type from that observed for $A = \text{K}, \text{Rb}$ in their work, and for $A = \text{NH}_4$ here. Devi & Vidyasagar (2000) utilized $(\text{NH}_4)_2\text{HPO}_4$ as the phosphate source in their high-temperature preparations of $A_3\text{Al}_2(\text{PO}_4)_3$, but did not obtain $(\text{NH}_4)_3\text{Al}_2(\text{PO}_4)_3$, likely due to the volatility of NH_3 at high temperatures.

As in the K and Rb forms of the $A_3\text{Al}_2(\text{PO}_4)_3$ series, aluminum and phosphorus are both tetrahedrally coordinated and connected through corners throughout the $(\text{NH}_4)_3\text{Al}_2(\text{PO}_4)_3$ structure. The NH_4^+ cations reside in a channel along the *c*-axis direction made from a 12 *T*-site ring of alternating AlO_4 and PO_4 tetrahedra (Fig. 2). The NH_4^+ groups occupy the available space and none of the ionic liquid

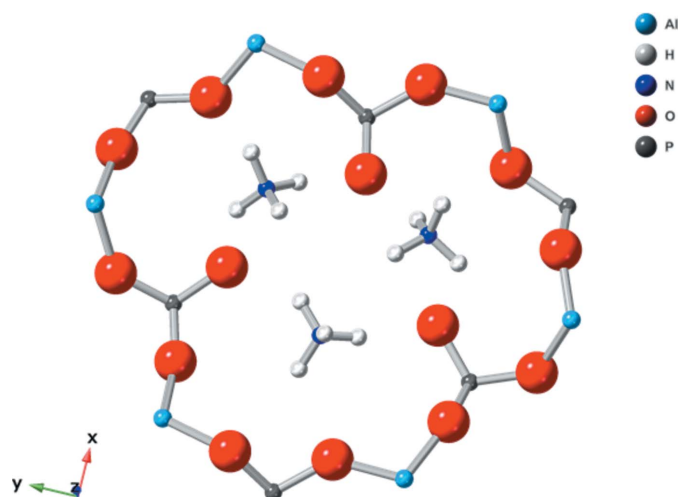


Figure 2
Ball and stick representation of $(\text{NH}_4)_3\text{Al}_2(\text{PO}_4)_3$ showing the 12-membered ring with three phosphate groups protruding inward with close contact to ammonium cations.

Table 2
Key atomic distances (Å) in related $A_3Al_2(PO_4)_3$ structures.

Compound	O11–A1	O11–A2	O11–A3	O11–P3	Reference
$(NH_4)_3Al_2(PO_4)_3$	3.162	2.818	2.727	1.487	This work
SIZ-2 ($A = NH_4$)	3.090	2.834	2.688	1.496	Cooper <i>et al.</i> (2004)
$K_3Al_2(PO_4)_3$	2.754	2.824	2.722	1.487	Devi & Vidyasagar (2000)
$K_3Al_2(AsO_4)_2(PO_4)$	3.025	2.743	2.621	1.673	Boughzala <i>et al.</i> (1997)

For each of the compounds, the atomic numbering scheme of the current $(NH_4)_3Al_2(PO_4)_3$ refinement has been utilized. For the first two compounds, $A = NH_4$, while for the second two, $A = K$. For the As-containing compound, the P3 site is reported to have the highest occupancy of As at 0.86.

solvent is present within the pores of the $(NH_4)_3Al_2(PO_4)_3$ framework. Without the NH_4^+ groups, the structure would have 24% void volume. The framework is triply negatively charged and charge-balanced by the ammonium cations. Three of the six phosphate groups in the ring protrude inward such that the closest contact distance between the H atom of an ammonium group and the O atom of the nearest phosphate is between 1.83 and 1.87 Å, indicating significant hydrogen-bonding interactions. The full range of H···O hydrogen-bond lengths is between 1.83 and 1.97 Å (Table 1).

Crystallizing in space-group type $Pna2_1$, $(NH_4)_3Al_2(PO_4)_3$ is isostructural to, but with a slightly larger unit cell than the K form synthesized by Devi & Vidyasagar (2000). Lattice expansion of ~ 0.1 – 0.2 Å occurs along each of the three axes, leading to an overall 6.6% increase in cell volume from 1245 to 1327 Å³. A lattice expansion is no surprise as the ionic radius of NH_4^+ is between 1.4 and 1.67 Å depending on the coordination number (Sidey, 2016). This is slightly larger than the reported 1.37 to 1.55 Å range for K^+ (Shannon, 1976). Much of the relative lattice expansion for $(NH_4)_3Al_2(PO_4)_3$ occurs along the a and c axes. Tilting of tetrahedra accounts for a significantly smaller expansion of the long b axis. In addition, an isostructural K/As form is also known where two-thirds of the phosphate groups have been replaced by arsenate (Boughzala *et al.*, 1997). Arsenate included on the phosphate sites increases the cell volume to 1307 Å³, just smaller than that recorded here for $(NH_4)_3Al_2(PO_4)_3$. The pure arsenate form $K_3Al_2(AsO_4)_3$ was reported by Stöger & Weil (2012),

which has a cell volume of 1328 Å³, essentially equivalent to that here.

An overlay plot of atomic positions of $(NH_4)_3Al_2(PO_4)_3$ (red) versus SIZ-2 (blue) shows that although the independent refinements of the two $(NH_4)_3Al_2(PO_4)_3$ materials were performed *via* different methods at different temperatures, most atom positions are similar, with no more than about 0.004 fractional position differences along the a or c axes (for these axes, about 0.03–0.04 Å, Fig. 3). One area stands out in the $A_3Al_2(PO_4)_3$ series. Fig. 4 shows the key area surrounding O11 where the largest position movement is observed in the two independent refinements of $(NH_4)_3Al_2(PO_4)_3$.

The P3–O11 bond is always among the shortest P–O bonds found in the crystal structure, here at 1.487 (5) Å. Two clusters of P–O bond lengths occur; one at about 1.49 Å and another at 1.55 Å. These distances are relatively typical for aluminophosphates (Richardson & Vogt, 1992; Wei *et al.*, 2012). Each of the O atoms protruding into the pore possess short P–O bonds and hydrogen bonds to two ammonium ions (Table 1). In particular, N2, N3, O11, and P3 are effectively in a plane so that with the hydrogen bonding present in our refined model from N3 and N2 through the attached H atoms to O11, O11 moves closer to P3 while N2 and N3 move slightly further away *versus* the positions in the SIZ-2 refinement. Table 2 shows respective O–A and P–O distances for the

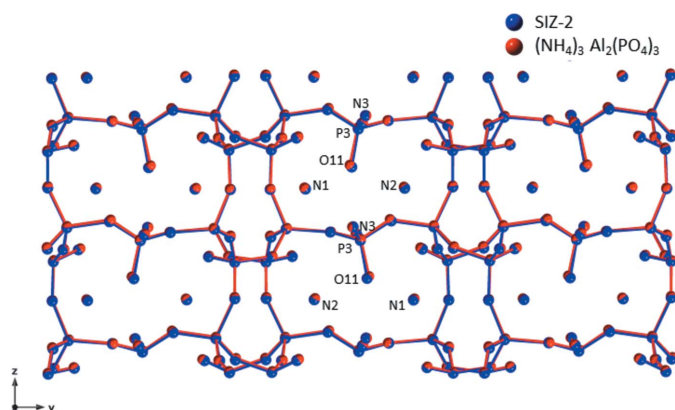


Figure 3
Atomic position overlay plot of SIZ-2 (blue) and $(NH_4)_3Al_2(PO_4)_3$ (red) showing that most atom positions are within 0.03 Å of each other. The most significant difference is in the O11 position.

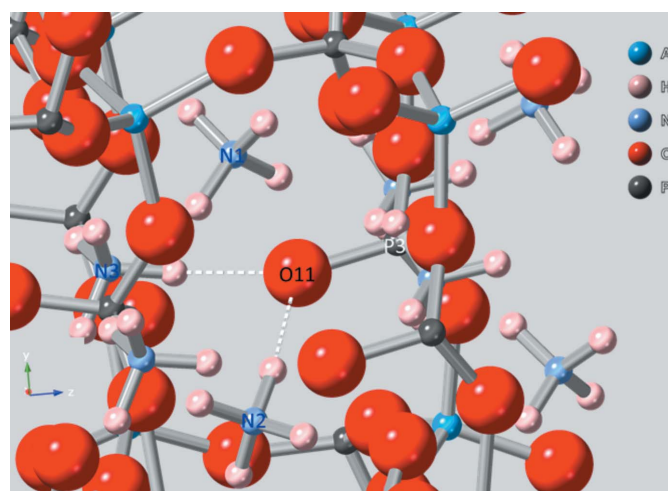


Figure 4
Ball and stick representation of the key area surrounding O11 where the largest position movement takes place in the two independent refinements of $(NH_4)_3Al_2(PO_4)_3$.

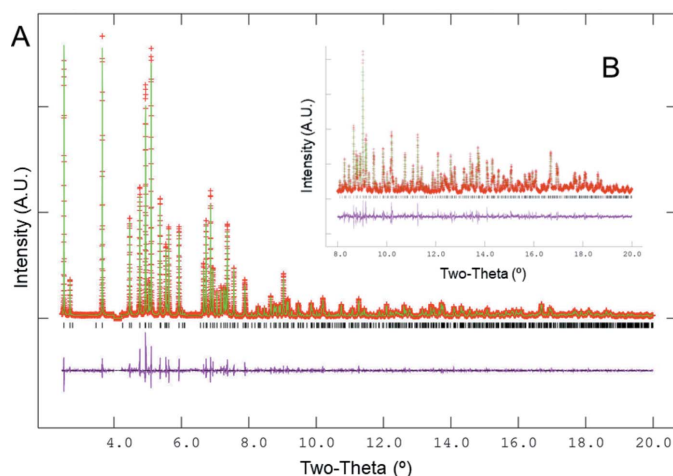


Figure 5
XRD pattern ($\lambda = 0.373811 \text{ \AA}$) of $(\text{NH}_4)_3\text{Al}_2(\text{PO}_4)_3$ synthesized ionothermally in ethyl tributylphosphonium diethylphosphate and Rietveld residuals following structure refinement. Part A shows the fit to the overall pattern, and inset B shows the fit to high-angle regions.

four isostructural $A_3\text{Al}_2(\text{PO}_4)_3$ compounds. Other bond lengths and angles are otherwise relatively unremarkable *versus* other members of the structural class although we note that As/P–O distances are longer than P–O as expected.

$\text{Rb}_3\text{Al}_2(\text{PO}_4)_3$ is structurally related to the NH_4 and K forms, but crystallizes in a higher symmetry space-group type ($Cmc2_1$), accompanied with higher overall coordination numbers around Rb^+ and a mirror plane perpendicular to a . The ionic radius of Rb^+ is similar to that of NH_4^+ , reported as 1.52–1.63 Å (Shannon, 1976). Lithium and cesium forms of the series have not yet been synthesized, likely because of the relatively small and large, respectively, ionic radii *versus* those of the fitting A cations. Our initial attempts at ion-exchange of $(\text{NH}_4)_3\text{Al}_2(\text{PO}_4)_3$ with LiNO_3 or CsNO_3 in aqueous solution to form the Li or Cs form failed, with partial structural degradation and no ion-exchange observed.

3. Synthesis and crystallization

In a typical preparation, 1.65 g $(\text{NH}_4)_2\text{HPO}_4$ was added to a 125 ml polytetrafluoroethene (PTFE) lined autoclave containing 24.02 g of ethyl tri(butyl)phosphonium diethyl phosphate. The mixture was stirred at room temperature for 2 min. To this mixture were added 0.49 g of $\text{Al}(\text{OH})_3$, and the contents were stirred at room temperature for 2 min. The contents of the autoclave were digested at 423 K for 24 h prior to isolating the product by filtration. Analytical results show this material has a molar ratio Al:P of 0.725. The X-ray diffraction pattern is shown in Fig. 5. Scanning electron microscopy (SEM) revealed agglomerated stacks of irregularly shaped blocky crystals of from 500 nm to 2–4 µm in length (Fig. 6). Calcination of $(\text{NH}_4)_3\text{Al}_2(\text{PO}_4)_3$ at temperatures of 773 K or higher causes the formation of an AlPO_4

Table 3
Experimental details.

Crystal data	
Chemical formula	$(\text{NH}_4)_3\text{Al}_2(\text{PO}_4)_3$
M_r	392.99
Crystal system, space group	Orthorhombic, $Pna2_1$
Temperature (K)	100
a, b, c (Å)	8.98884 (6), 17.01605 (10), 8.67653 (5)
V (Å ³)	1327.11 (2)
Z	4
Radiation type	Synchrotron, $\lambda = 0.373811 \text{ \AA}$
μ (mm ⁻¹)	0.12
Specimen shape, size (mm)	Cylinder, 0.70 × 0.70
Data collection	
Diffractometer	11BM synchrotron
Specimen mounting	Capillary
Data collection mode	Transmission
Scan method	Continuous
2θ values (°)	$2\theta_{\min} = 2.45$, $2\theta_{\max} = 20$, $2\theta_{\text{step}} = 0.001$
Refinement	
R factors and goodness of fit	$R_p = 0.082$, $R_{wp} = 0.101$, $R_{\text{exp}} = 0.060$, $R(F^2) = 0.03552$, $\chi^2 = 2.856$
No. of parameters	95
No. of restraints	20
H-atom treatment	H atoms treated by a mixture of independent and constrained refinement
$(\Delta/\sigma)_{\max}$	0.17

Computer programs: local program at 11BM, *GSAS* (Larson & Von Dreele, 2000), coordinates from an isotopic structure, *CrystalMaker* (Palmer, 2005), *pubCIF* (Westrip, 2010).

phase with a tridymite-type structure. Ethyl tributyl phosphonium diethyl phosphate (Cyphos 169) was acquired from Cytec; aluminum hydroxide was acquired from Pfaltz and Bauer.

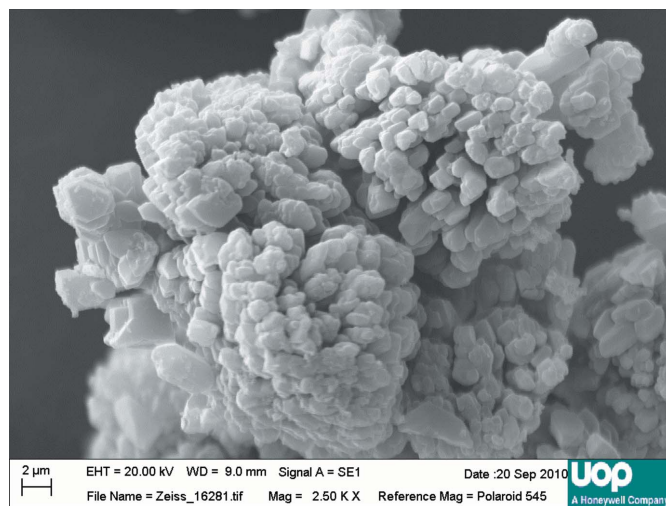


Figure 6
SEM image of polycrystalline $(\text{NH}_4)_3\text{Al}_2(\text{PO}_4)_3$ synthesized ionothermally in ethyl tributylphosphonium diethyl phosphate and used for structure refinement.

4. Refinement

Crystal data, data collection and structure refinement details are summarized in Table 3. Following initial survey scans on in-house Cu source powder XRD instruments, final data were acquired from samples packed in thin glass capillaries on 11-BM at the Advanced Photon Source at Argonne National Laboratory. Starting atomic positions for the refinement were adapted from the literature examples. Starting positions for the ammonium cations were located in a difference-Fourier map and subsequently refined using GSAS (Larson & Von Dreele, 2000) as tetrahedral rigid bodies with N–H bond lengths held at 0.9526 Å and tetrahedrality enforced, leading to H···H distances of 1.5556 Å. No soft constraints were applied to the framework positions. All atoms in the structure were refined with a common U_{iso} parameter. Two low-intensity reflections in the region $4.00\text{--}4.22^\circ/2\theta$ were excluded from the refinement as belonging to an impurity phase after assessment of multiple $(\text{NH}_4)_3\text{Al}_2(\text{PO}_4)_3$ batches. Refinement trials with a higher symmetry model (space-group type $Cmc2_1$) were attempted but showed poor agreement with the experimental data, with $R_{\text{wp}} > 0.16$.

Acknowledgements

We thank UOP for funding and allowing this publication. Use of the Advanced Photon Source at Argonne National Laboratory was supported by the US Department of Energy, Office of Science, Office of Basic Energy Sciences, under Contract No. DE-AC02-06CH11357. We acknowledge E. Fulmer, C. L. Nicholas and S. T. Wilson for helpful discussions and J. F. Kotek and A. Stolarski for the ICP and SEM results.

Funding information

Funding for this research was provided by: UOP LLC.

References

- Boughzala, H., Driss, A. & Jouini, T. (1997). *Acta Cryst.* **C53**, 3–5.
- Byrne, P. J., Warren, J. E., Morris, R. E. & Ashbrook, S. E. (2009). *Solid State Sci.* **11**, 1001–1006.
- Cooper, E. R., Andrews, C. D., Wheatley, P. S., Webb, P. B., Wormald, P. & Morris, R. E. (2004). *Nature*, **430**, 1012–1016.
- Das, S. K., Bhunia, M. K. & Bhaumik, A. (2012). *Microporous Mesoporous Mater.* **155**, 258–264.
- Devi, R. N. & Vidyasagar, K. (2000). *Inorg. Chem.* **39**, 2391–2396.
- Larson, A. C. & Von Dreele, R. B. (2000). *General Structure Analysis System (GSAS)*. Report LAUR, 86–748 Los Alamos National Laboratory, New Mexico, USA.
- Li, Y., Yu, J. & Xu, R. (2019). *URL of ALPO database (freely accessible)*: <http://mezeopor.jlu.edu.cn/alpo/alpo.jsp>
- Ma, H., Tian, Z., Xu, R., Wang, B., Wei, Y., Wang, L., Xu, Y., Zhang, W. & Lin, L. (2008). *J. Am. Chem. Soc.* **130**, 8120–8121.
- Medina, M. E., Iglesias, M., Gutiérrez-Puebla, E. & Monge, M. A. (2004). *J. Mater. Chem.* **14**, 845–850.
- Morris, R. E. (2009). *Chem. Commun.* pp. 2990–2998.
- Oliver, S., Kuperman, A., Lough, A. & Ozin, G. A. (1996). *Chem. Commun.* pp. 1761–1762.
- Palmer, D. (2005). *CrystalMaker*. CrystalMaker Software Ltd, Yarnton, England.
- Parnham, E. & Morris, R. E. (2007). *Acc. Chem. Res.* **40**, 1005–1013.
- Richardson, J. W. & Vogt, E. T. C. (1992). *Zeolites*, **12**, 13–19.
- Shannon, R. D. (1976). *Acta Cryst.* **A32**, 751–767.
- Sidey, V. (2016). *Acta Cryst.* **B72**, 626–633.
- Stöger, B. & Weil, M. (2012). *Acta Cryst.* **E68**, i15.
- Vaughan, D. E. W., Yennawar, H. P. & Perrotta, A. J. (2012). *Microporous Mesoporous Mater.* **153**, 18–23.
- Wei, Y., Marler, B., Zhang, L., Tian, Z., Graetsch, H. & Gies, H. (2012). *Dalton Trans.* **41**, 12408–12415.
- Westrip, S. P. (2010). *J. Appl. Cryst.* **43**, 920–925.
- Wilson, S. T. (2007). *Introduction to Zeolite Science and Practice*, 3rd ed, edited by J. Čejka, H. van Bekkum, A. Corma, & F. Schüth, ch. 4, pp. 105–135. Amsterdam: Elsevier.
- Wilson, S. T., Lok, B. M., Messina, C. A., Cannan, T. R. & Flanigen, E. M. (1982). *J. Am. Chem. Soc.* **104**, 1146–1147.
- Xing, H., Li, J., Yan, W., Chen, P., Jin, Z., Yu, J., Dai, S. & Xu, R. (2008). *Chem. Mater.* **20**, 4179–4181.
- Xing, H., Li, Y., Su, T., Xu, J., Yang, W., Zhu, E., Yu, J. & Xu, R. (2010). *Dalton Trans.* **39**, 1713–1715.
- Yu, J. & Xu, R. (2006). *Chem. Soc. Rev.* **35**, 593–604.

supporting information

Acta Cryst. (2019). E75, 1897-1901 [https://doi.org/10.1107/S2056989019015330]

Structure refinement of $(\text{NH}_4)_3\text{Al}_2(\text{PO}_4)_3$ prepared by ionothermal synthesis in phosphonium based ionic liquids – a redetermination

Christopher P. Nicholas, John P.S. Mowat and Robert W. Broach

Computing details

Data collection: local program at 11BM; data reduction: *GSAS* (Larson & Von Dreele, 2000); program(s) used to solve structure: coordinates from an isotypic structure; program(s) used to refine structure: *GSAS* (Larson & Von Dreele, 2000); molecular graphics: *CrystalMaker* (Palmer, 2005); software used to prepare material for publication: *pubCIF* (Westrip, 2010).

Triammonium dialuminium tris(phosphate)

Crystal data

$(\text{NH}_4)_3\text{Al}_2(\text{PO}_4)_3$

$M_r = 392.99$

Orthorhombic, *Pna*2₁

Hall symbol: P 2c -2n

$a = 8.98884$ (6) Å

$b = 17.01605$ (10) Å

$c = 8.67653$ (5) Å

$V = 1327.11$ (2) Å³

$Z = 4$

Synchrotron radiation, $\lambda = 0.373811$ Å

$\mu = 0.12$ mm⁻¹

$T = 100$ K

white

cylinder, 0.70 × 0.70 mm

Data collection

11BM synchrotron

diffractometer

Specimen mounting: capillary

Data collection mode: transmission

Scan method: continuous

$2\theta_{\min} = 2.45^\circ$, $2\theta_{\max} = 20^\circ$, $2\theta_{\text{step}} = 0.001^\circ$

Refinement

Least-squares matrix: full

$R_p = 0.082$

$R_{wp} = 0.101$

$R_{exp} = 0.060$

$R(F^2) = 0.03552$

49495 data points

Profile function: CW Profile function number 4

with 18 terms Pseudovoigt profile coefficients as parameterized in P. Thompson, D.E. Cox & J.B. Hastings (1987). J. Appl. Cryst.,20,79-83. Asymmetry correction of L.W. Finger, D.E. Cox & A. P. Jephcoat (1994). J. Appl. Cryst.,27,892-900. Microstrain broadening by P.W. Stephens, (1999). J. Appl. Cryst.,32,281-289. #1(GU) = 1.163 #2(GV) = -0.126 #3(GW) = 0.063 #4(GP) = 0.000 #5(LX) = 0.143 #6(ptec) = -0.01 #7(trns) = 0.00 #8(shft) = 0.0000 #9(sfec) = 0.00 #10(S/L) = 0.0011 #11(H/L) = 0.0011 #12(eta) = 0.7694 #13(S400) = 1.1E-01 #14(S040) = 2.8E-03 #15(S004) = 1.0E-01 #16(S220) = 1.3E-02 #17(S202) = -9.0E-03 #18(S022) = 6.9E-03 Peak tails are ignored where the intensity is below 0.0010 times the peak Aniso. broadening axis 1.0 0.0 0.0

95 parameters

20 restraints

H atoms treated by a mixture of independent and constrained refinement

$(\Delta/\sigma)_{max} = 0.17$

Background function: GSAS Background

function number 1 with 11 terms. Shifted Chebyshev function of 1st kind 1: 111.086 2: -42.2923 3: 17.4011 4: -1.76183 5: -7.25556 6: 2.97020 7: 2.60010 8: -3.84672 9: 5.91765 10: -3.48127 11: 1.19076

Fractional atomic coordinates and isotropic or equivalent isotropic displacement parameters (\AA^2)

	x	y	z	U_{iso}^*/U_{eq}
P1	0.1689 (3)	0.21458 (16)	-0.0138 (5)	0.0086 (3)*
P2	0.3100 (3)	0.29952 (16)	0.4927 (5)	0.0086 (3)*
P3	0.2594 (3)	0.5033 (2)	0.0861	0.0086 (3)*
Al1	0.3631 (4)	0.33375 (18)	0.1361 (5)	0.0086 (3)*
Al2	0.1295 (4)	0.17048 (19)	0.6462 (5)	0.0086 (3)*
O1	0.2886 (7)	0.1552 (3)	0.0117 (8)	0.0086 (3)*
O2	0.0384 (8)	0.2046 (3)	0.1014 (8)	0.0086 (3)*
O3	0.2289 (7)	0.3006 (3)	0.0100 (8)	0.0086 (3)*
O4	0.1017 (7)	0.2138 (4)	0.8252 (8)	0.0086 (3)*
O5	0.1953 (7)	0.3602 (3)	0.5464 (8)	0.0086 (3)*
O6	0.4625 (7)	0.3234 (3)	0.5425 (8)	0.0086 (3)*
O7	0.2776 (8)	0.2165 (3)	0.5518 (7)	0.0086 (3)*
O8	0.3087 (7)	0.2962 (4)	0.3126 (8)	0.0086 (3)*
O9	0.1072 (5)	0.4838 (3)	0.1404 (8)	0.0086 (3)*
O10	0.3228 (7)	0.5700 (4)	0.1747 (7)	0.0086 (3)*
O11	0.2604 (6)	0.5218 (3)	0.9186 (6)	0.0086 (3)*
O12	0.3716 (7)	0.4348 (3)	0.1188 (9)	0.0086 (3)*

N1	0.0164 (8)	0.3978 (4)	0.8194 (9)	0.0086 (3)*
H11	0.076 (5)	0.425 (3)	0.893 (4)	0.0086 (3)*
H12	-0.058 (4)	0.368 (3)	0.871 (5)	0.0086 (3)*
H13	0.077 (5)	0.364 (2)	0.760 (5)	0.0086 (3)*
H14	-0.030 (5)	0.435 (2)	0.753 (5)	0.0086 (3)*
N2	0.9630 (8)	0.3743 (4)	0.3168 (9)	0.0086 (3)*
H21	1.036 (4)	0.363 (3)	0.393 (5)	0.0086 (3)*
H22	0.915 (6)	0.3268 (16)	0.287 (6)	0.0086 (3)*
H23	1.009 (5)	0.397 (3)	0.229 (4)	0.0086 (3)*
H24	0.891 (5)	0.410 (3)	0.358 (6)	0.0086 (3)*
N3	0.6786 (6)	0.4917 (4)	0.1118 (7)	0.0086 (3)*
H31	0.755 (4)	0.530 (2)	0.095 (6)	0.0086 (3)*
H32	0.668 (5)	0.483 (3)	0.2196 (14)	0.0086 (3)*
H33	0.704 (5)	0.4438 (18)	0.062 (5)	0.0086 (3)*
H34	0.587 (3)	0.511 (3)	0.071 (5)	0.0086 (3)*

Geometric parameters (Å, °)

P1—A11	2.975 (5)	O3—P1	1.573 (6)
P1—A12 ⁱ	3.064 (5)	O3—A11	1.724 (7)
P1—O1	1.493 (6)	O4—P1 ^{iv}	1.522 (7)
P1—O2	1.550 (7)	O4—A12	1.737 (7)
P1—O3	1.573 (6)	O5—P2	1.532 (6)
P1—O4 ⁱ	1.522 (7)	O5—H21 ^{viii}	1.953 (13)
P2—A12	3.038 (4)	O5—H31 ^{ix}	1.97 (3)
P2—O5	1.532 (6)	O6—P2	1.493 (7)
P2—O6	1.493 (7)	O6—A12 ⁱⁱⁱ	1.753 (7)
P2—O7	1.532 (6)	O7—P2	1.532 (6)
P2—O8	1.563 (6)	O7—A12	1.748 (7)
P3—A11	3.062 (5)	O8—P2	1.563 (6)
P3—A12 ⁱⁱ	3.060 (5)	O8—A11	1.730 (7)
P3—O9	1.484 (5)	O9—P3	1.484 (5)
P3—O10	1.485 (6)	O9—H14 ^x	1.828 (10)
P3—O11 ⁱ	1.487 (5)	O9—H23 ^{viii}	1.88 (3)
P3—O12	1.567 (6)	O10—P3	1.485 (6)
A11—P1	2.975 (5)	O10—A12 ⁱⁱ	1.780 (7)
A11—P3	3.062 (5)	O11—P3 ^{iv}	1.487 (5)
A11—O2 ⁱⁱⁱ	1.732 (7)	O11—H24 ^{ix}	1.868 (10)
A11—O3	1.724 (7)	O11—H32 ^{ix}	1.84 (2)
A11—O8	1.730 (7)	O12—P3	1.567 (6)
A11—O12	1.727 (6)	O12—A11	1.727 (6)
A12—P1 ^{iv}	3.064 (5)	N1—H11	0.9526 (1)
A12—P2	3.038 (4)	N1—H12	0.9526 (1)
A12—P3 ^v	3.060 (5)	N1—H13	0.9526 (1)
A12—O4	1.737 (7)	N1—H14	0.9526
A12—O6 ^{vi}	1.753 (7)	N2—H21	0.9526 (1)
A12—O7	1.748 (7)	N2—H22	0.9526 (1)
A12—O10 ^v	1.780 (7)	N2—H23	0.9526 (1)

O1—P1	1.493 (6)	N2—H24	0.9526 (1)
O1—H12 ^{vii}	1.88 (2)	N3—H31	0.9526 (1)
O1—H33 ^{vi}	1.897 (15)	N3—H32	0.9526 (1)
O2—P1	1.550 (7)	N3—H33	0.9526 (1)
O2—Al1 ^{vi}	1.732 (7)	N3—H34	0.9526 (1)
O1—P1—O2	112.1 (4)	O6 ^{vi} —Al2—O10 ^v	109.6 (3)
O1—P1—O3	111.3 (4)	O7—Al2—O10 ^v	108.1 (3)
O1—P1—O4 ⁱ	114.6 (4)	P1—O2—Al1 ^{vi}	147.3 (5)
O2—P1—O3	106.1 (4)	P1—O3—Al1	128.9 (4)
O2—P1—O4 ⁱ	106.9 (4)	P1 ^{iv} —O4—Al2	140.1 (4)
O3—P1—O4 ⁱ	105.4 (4)	P2—O6—Al2 ⁱⁱⁱ	161.9 (5)
O5—P2—O6	110.3 (4)	P2—O7—Al2	135.6 (5)
O5—P2—O7	113.1 (4)	P2—O8—Al1	150.4 (4)
O5—P2—O8	108.9 (4)	P3—O10—Al2 ⁱⁱ	139.0 (5)
O6—P2—O7	109.2 (4)	P3—O12—Al1	136.7 (5)
O6—P2—O8	107.8 (4)	H11—N1—H12	109.4713 (9)
O7—P2—O8	107.4 (4)	H11—N1—H13	109.4719 (6)
O9—P3—O10	111.1 (4)	H11—N1—H14	109.4706
O9—P3—O11 ⁱ	111.3 (4)	H12—N1—H13	109.4715 (1)
O9—P3—O12	111.7 (4)	H12—N1—H14	109.4704
O10—P3—O11 ⁱ	110.0 (4)	H13—N1—H14	109.4715 (5)
O10—P3—O12	103.2 (3)	H21—N2—H22	109.4716 (7)
O11 ⁱ —P3—O12	109.3 (4)	H21—N2—H23	109.4710 (4)
O2 ⁱⁱⁱ —Al1—O3	113.8 (4)	H21—N2—H24	109.4716 (4)
O2 ⁱⁱⁱ —Al1—O8	105.8 (4)	H22—N2—H23	109.4707
O2 ⁱⁱⁱ —Al1—O12	108.6 (4)	H22—N2—H24	109.4717 (8)
O3—Al1—O8	104.1 (3)	H23—N2—H24	109.4706 (7)
O3—Al1—O12	107.6 (4)	H31—N3—H32	109.4709
O8—Al1—O12	117.2 (4)	H31—N3—H33	109.4710 (5)
O4—Al2—O6 ^{vi}	108.1 (3)	H31—N3—H34	109.4709 (1)
O4—Al2—O7	109.8 (3)	H32—N3—H33	109.4717
O4—Al2—O10 ^v	108.5 (4)	H32—N3—H34	109.472
O6 ^{vi} —Al2—O7	112.6 (4)	H33—N3—H34	109.4709

Symmetry codes: (i) $x, y, z-1$; (ii) $-x+1/2, y+1/2, z-1/2$; (iii) $x+1/2, -y+1/2, z$; (iv) $x, y, z+1$; (v) $-x+1/2, y-1/2, z+1/2$; (vi) $x-1/2, -y+1/2, z$; (vii) $x+1/2, -y+1/2, z-1$; (viii) $x-1, y, z$; (ix) $-x+1, -y+1, z+1/2$; (x) $-x, -y+1, z-1/2$.

Hydrogen-bond geometry ($\text{\AA}, ^\circ$)

$D-H\cdots A$	$D-H$	$H\cdots A$	$D\cdots A$	$D-H\cdots A$
N1—H11 \cdots O9 ^{iv}	0.95 (4)	2.39 (4)	3.250 (10)	151 (3)
N1—H11 \cdots O11	0.95 (4)	2.35 (5)	3.163 (8)	143 (3)
N1—H12 \cdots O1 ^{xi}	0.95 (4)	1.88 (4)	2.791 (10)	159 (3)
N1—H13 \cdots O5	0.95 (4)	2.14 (4)	2.934 (10)	141 (3)
N1—H14 \cdots O9 ^{xii}	0.95 (4)	1.83 (4)	2.776 (9)	173 (3)
N2—H21 \cdots O5 ^{xiii}	0.95 (4)	1.96 (4)	2.896 (10)	170 (4)
N2—H22 \cdots O8 ⁱⁱⁱ	0.95 (4)	2.31 (3)	3.216 (10)	158 (4)
N2—H23 \cdots O9 ^{xiii}	0.95 (4)	1.89 (5)	2.738 (9)	148 (4)

N2—H24···O11 ^{xiv}	0.96 (4)	1.86 (4)	2.818 (9)	174 (5)
N3—H31···O5 ^{xiv}	0.96 (4)	1.97 (4)	2.821 (9)	147 (3)
N3—H32···O11 ^{xiv}	0.952 (15)	1.85 (2)	2.728 (8)	153 (4)
N3—H33···O1 ⁱⁱⁱ	0.95 (3)	1.90 (3)	2.823 (9)	164 (4)
N3—H34···O12	0.96 (3)	2.37 (4)	2.925 (8)	117 (4)

Symmetry codes: (iii) $x+1/2, -y+1/2, z$; (iv) $x, y, z+1$; (xi) $x-1/2, -y+1/2, z+1$; (xii) $-x, -y+1, z+1/2$; (xiii) $x+1, y, z$; (xiv) $-x+1, -y+1, z-1/2$.